

Integration of CHIME into the NANOGrav Pulsar Timing Array

Gabriella Agazie for the CHIME/Pulsar and NANOGrav Collaborations

Center for Gravitation, Cosmology, and Astrophysics, Dept. of Physics, University of Wisconsin-Milwaukee, Milwaukee, WI, USA

Abstract

The North American Nanohertz Observatory for Gravitational Waves (NANOGrav) pulsar timing array (PTA) is constructed from long-term timing campaigns of a large number of millisecond pulsars (MSPs). Wideband timing techniques have been used in NANOGrav datasets since the release of the 12.5-yr dataset and have proved useful for studying time-varying dispersion measure, which can limit timing precision. We are also limited by the fact that NANOGrav observations occur on a monthly cadence. The Canadian Hydrogen Intensity Mapping Experiment (CHIME) Telescope has been observing NANOGrav MSPs at 600 MHz (400 MHz bandwidth) with nearly daily cadence for the past four years. In this paper we report the results of combining one year of CHIME data with NANOGrav data taken over the same time period for four MSPs: PSR J0030+0451, PSR J0613–0200, PSR J0740+6620, and PSR J2145–0750.

1. Introduction

The North American Nanohertz Observatory for Gravitational Waves (NANOGrav) conducts high-precision timing over long timescales of a large number of millisecond pulsars (MSPs). These MSPs are components of a pulsar timing array (PTA) that can be used to directly detect and study nHz-frequency gravitational waves by looking at correlated perturbations in pulse times of arrival (TOAs). The first evidence of the detection of the gravitational wave background using PTAs was recently published by the NANOGrav collaboration in conjunction with other PTA collaborations across the globe (Agazie, Anumarpudi, et al., 2023).

Pulsars are a class of rapidly spinning and highly magnetized neutron star characterized by the emission of electromagnetic radiation from both magnetic poles. This radiation, which is most easily detected at radio wavelengths, is observed as a series of pulses separated in time by the rotation period of the pulsar (Lorimer & Kramer, 2012; Lorimer, 2008). Pulsar timing can be used to infer intrinsic and extrinsic characteristics of the source (Lorimer, 2008; Agazie, Alam, et al., 2023). This involves taking TOA measurements from observations, comparing them to models of pulsar rotation called timing ephemerides, and computing timing residuals. Timing residuals represent the difference between the pulse phase of rotation of an observed TOA, and the pulse phase a timing model predicts. An accurate timing ephemeris produces timing residuals that are small and consistent with zero relative to TOA uncertainties. Examples of intrinsic characteristics used in pulsar timing include spin period and spin period derivative. Extrinsic, astrometric parameters such as sky position, parallax and proper motion are important for studying spacial correlations in gravitational wave searches (Agazie, Anumarpudi, et al., 2023; Arzoumanian et al., 2020). Pulsars in binaries have measurable Keplerian parameters, and in some cases we can also measure relativistic post-Keplerian binary parameters. Both are extremely useful for placing limits on neutron star masses and orbital orientation, which are an important astrophysical constraints on the poorly understood nuclear equation of state (Burgio et al., 2021).

When timing pulsars, we can expect some evolution of the pulse profile shape as a function of frequency caused by intrinsic changes in the pulsar magnetosphere, and extrinsic effects caused by interstellar scattering and frequency-dependent dispersion measure (DM). When measuring TOAs, especially from MSPs, this profile evolution can significantly impact timing precision by introducing frequency dependent time delays (Lorimer & Kramer, 2012). Traditional narrowband (NB) timing techniques attempt to capture frequency-dependent trends by subbanding individual observations into frequency bins of ~ 10 MHz width and calculating one TOA from each subband using the same 1-D pulse profile template that has been averaged over frequency (Agazie, Alam, et al., 2023; Alam et al., 2021a). This method

requires many TOAs to be calculated from a single observation, and introduces statistical biases that require correction through the inclusion of arbitrary frequency-dependent parameters (NANOGrav Collaboration et al., 2015).

Wideband (WB) timing is a relatively recently developed technique in which a single TOA and simultaneous DM measurement from every observation using a 2-D ‘portrait’ which captures the evolution of pulse profile in frequency and phase. The portrait is made by aligning and averaging all available data in phase and frequency to compute a data template with a high signal-to-noise ratio (S/N). This template is then de-noised using wavelet smoothing, and a model portrait is derived using principal component analysis and spline interpolation (Pennucci, 2019). Calculating TOAs with this method eliminates some of the biases we see in NB timing and means that WB TOAs have much greater precision than NB TOAs since only one TOA measurement need be made from a single observation. This can result in greater timing precision with WB timing vs NB (Agazie, Alam, et al., 2023; Alam et al., 2021b).

The Canadian Hydrogen Intensity Mapping Experiment (CHIME) Telescope is a drift scan radio telescope that has been observing sources in the NANOGrav pulsar timing array (PTA) for the past four years (The CHIME Collaboration et al., 2022; CHIME/Pulsar Collaboration et al., 2021; Good, 2021). In this paper, we present results of data combination using WB timing techniques of CHIME data with the NANOGrav 15 year dataset (NG15) for four pulsars: PSR J0030+0451, PSR J0613–0200, PSR J0740+6620, and PSR J2145–0750. In Section 2 we describe data reduction and timing techniques. Results are presented in Section 3, and discussion of results in Section 4.

2. Methods

The analysis reported in this paper focuses on data taken between April 2019 and March 2020. This 11-month time period is the overlap period between the beginning of CHIME timing observations on NANOGrav sources and the end date of data collection for NG15 (Agazie, Alam, et al., 2023).

2.1. NANOGrav Data NG15 data was collected at both the 100-m Robert C. Byrd Green Bank Telescope (GBT) and the 305-m William E. Gordon Telescope of the Arecibo Observatory (AO) at monthly cadence. Data during our time period of interest was recorded with the Green Bank Ultimate Pulsar Processing Instrument (GUPPI) at the GBT and the Puerto Rican Ultimate Pulsar Processing Instrument (PUPPI) at AO. Both backends use 2048 phase bins and 1.56 MHz width frequency subbands. NG15 GUPPI data was taken with the 820 MHz and 1.4 GHz receivers with bandwidths of 186 MHz and 642 MHz respectively. NG15 PUPPI data was taken with the 430 MHz, 1400 MHz, and 2100 MHz receivers with bandwidths of 24 MHz, 460 MHz, and 603 MHz respectively. Typical observation durations were 25 minutes per receiver (NANOGrav Collaboration et al., 2015; Agazie, Alam, et al., 2023). Sources PSR J0613–0200, PSR J0740+6620, and PSR J2145–0750 only have GUPPI data, whereas PSR J0030+0451 only has PUPPI data.

Data reduction for all NG15 observations was done using the `nanopipe` software package and WB TOAs were calculated using the `pptoas.py` code in the `PulsePortraiture`¹ software package. Model portraits used to construct the 12.5-yr WB dataset were reused for the NG15 WB dataset (Agazie, Alam, et al., 2023).

2.2. CHIME Data CHIME observations for all four pulsars were taken in fold-mode at a central frequency of 600 MHz with a 400 MHz bandwidth and 1024 frequency channels. The CHIME/Pulsar backend collects 10 beam-formed voltages with time resolution of $2.56 \mu\text{s}$ and frequency resolution of 0.390625 MHz (The CHIME Collaboration et al., 2022). PSR J2145–0750 observations had 2048 phase bins whereas observations for PSR J0030+0451, PSR J0613–0200, and PSR J0740+6620 all had 1024 phase bins. Observations for all sources were taken at nearly daily cadence with an average duration of 10 minutes for PSR J2145–0750, 14 minutes for PSR J0030+0451 and PSR J0613–0200, and 34 minutes for PSR J0740+6620.

In order for this work to facilitate the eventual full integration of CHIME data into the NANOGrav PTA, we used a data reduction process similar to that used in `nanopipe`. For all sources we used the `PSRCHIVE` (van Straten et al., 2012) tool `pam` to conduct time and frequency averaging to end up with a single time sub-integration and 64 frequency sub-integrations. Radio frequency interference (RFI) was removed using `paz`.

¹<https://github.com/pennucci/PulsePortraiture>

WB model portraits currently are not accurate beyond the frequency range of the data portraits used to calculate the models, and do not inherently account for instrument offsets (Pennucci, 2019). Thus, we needed to make CHIME-specific model portraits for each source. This was done using the `PulsePortrait` software package. The `ppalign.py` tool was used to make data portraits by aligning and averaging all observations for a given source above an empirically determined S/N threshold. We used 20 for PSR J0030+451 and PSR J2145–0750, 30 for PSR J0740+6620, and 40 for PSR J0613–0200. The high data volume of CHIME data makes examining all individual observations difficult, so the S/N threshold is used to prevent the inclusion of noisy or marginal detections in the data portrait. Clean and high S/N data portraits are important to prevent noise from being artificially modeled as pulse profile evolution (Pennucci, 2019). We used `ppsspline.py` to make spline models of profile evolution which were then used to calculate WB TOAs using `pptoas.py`.

2.3. Timing Analysis Timing was done using the `PINT` software package ² (Luo et al., 2021). We started with the NG15 ephemerides and added additional JUMP and DMJUMP parameters for the CHIME receiver. These account for phase and DM offsets when doing timing with data taken at different receivers. To model time-varying DM we used the piece-wise constant DMX model (NANOGrav Collaboration et al., 2015). We fit for spin parameters for all sources, and for Keplerian binary parameters for those sources that are in binaries. The three binary pulsars in this analysis all have nearly circular orbits, so we used the ELL1 and ELL1H binary models. For both these models the parameters describing Keplerian motion are: orbital period (P_b), projected semi-major axis (x), epoch of ascending node of the binary system (T_{asc}), and the eccentricity parameters describing variations from circular motion (ϵ_1 and ϵ_2) (Lange et al., 2001; Freire & Wex, 2010). The ELL1H model used for PSR J2145-0750 only differs from the ELL1 model by the addition of relativistic Shapiro delay parameters, but we have left those frozen at the NG15 values for this work (Freire & Wex, 2010). The ELL1/ELL1H Keplerian parameters can be converted to traditional Keplerian parameters by the following equations:

$$e = \sqrt{\epsilon_1^2 + \epsilon_2^2} \quad \omega = \arctan(\epsilon_1/\epsilon_2) \quad T0 = T_{asc} + P_b \times \omega/2\pi$$

Where e is eccentricity, ω is longitude of periastron, and $T0$ is the epoch of periastron. We have done this conversion when reporting our timing results in Table 1. To combine our data with NG15 TOAs we iteratively added CHIME WB TOAs in small increments and re-fit for a new ephemeris. Since this analysis was done over a relatively short timescale, we froze all astrometric and relativistic parameters at the values in the NG15 timing ephemerides.

3. Results

PSR J0030+0451 is a 4.8-ms isolated MSP initially discovered during the Arecibo Drift Scan Survey (Lommen et al., 2000). Timing residuals for this source were nearly perfectly flat with minimal scattering, with CHIME TOAs on average having higher uncertainties and slightly more scattered residuals (Figure 1). Conversely, CHIME DM residuals had less scatter and, on average, smaller uncertainties than NG15. This source has comparable numbers of NG15 vs CHIME TOAs (Table 1). The timing ephemeris for this source had 503 degrees of freedom with a χ^2_{red} of 1.209, a weighted TOA RMS that was approximately 0.0086% of the pulsar spin period, and a weighted DM RMS that was 0.012% of the fiducial DM.

PSR J0613–0200 is a 3.1-ms MSP in a 1.2-day circular orbit about a $0.18 \pm 0.15 M_{\odot}$ companion (Lorimer et al., 1995). This source showed more scatter in CHIME TOA residuals vs NG15, but most CHIME residuals were still consistent with zero within the error bars. DM residuals appear to have comparable scatter between CHIME and NG15, although NG15 DM results seems to have higher uncertainties (Figure 2). This source and PSR J2145-0750 have nearly 10 times as many CHIME TOAs vs NG15 (Table 1). The timing ephemeris for this source had 373 degrees of freedom with a χ^2_{red} of 1.241. The weighted TOA RMS is approximately 0.014% of the pulsar spin period and the weighted DM RMS is 0.00057% of the fiducial DM. The χ^2_{red} is 1.241.

PSR J0740+6620 is a 2.9-ms, $2.08 \pm 0.07 M_{\odot}$ MSP in a 4.8-day circular orbit about a $0.253 \pm 0.006 M_{\odot}$ companion (Stovall et al., 2014; Fonseca et al., 2021). Timing and DM residuals for this source are relatively flat, and there is

²<https://github.com/nanograv/PINT>

Table 1: Timing results and statistics.

Parameter	PSR J0030+0451	PSR J0613–0200	PSR J0740+6620	PSR J2145–0750
P (s)	0.0048654532143 2827(2)	0.0030618440437 89666(3)	0.0028857364127 66008(2)	0.016052423680 2535(6)
\dot{P} (10^{-20} s s $^{-1}$)	1.0179(6)	0.9586(6)	1.2198(4)	2.93(2)
DM (pc cm $^{-3}$)	4.33306	38.7756	14.9638	9.00258
Binary Model	N/A	ELL1	ELL1	ELL1H
P_b (days)	N/A	1.19851255660(16)	4.7669446209(4)	6.838902511(4)
e	N/A	$4.1(12) \times 10^{-6}$	$5.94(2) \times 10^{-6}$	$1.945(7) \times 10^{-5}$
x (lt s)	N/A	1.09144117(6)	3.97755618(5)	10.1641109(3)
ω (deg)	N/A	31.7(16)	252.1(2)	200.8(2)
T_0 (MJD)	N/A	58824.814(5)	58837.7307(3)	58800.791(4)
Data Span (MJD)	58705 to 59068	58602 to 59047	58601 to 59072	58647 to 58943
N_{toa} (NG15/CHIME)	126/183	22/219	125/172	18/190
TOA RMS Residual (μ s)	0.415	0.436	0.467	0.923
DM RMS Residual (pc cm $^{-3}$)	0.00050	0.00022	0.00024	0.00086
χ^2_{red}	1.209	1.241	1.040	1.752

The PINT-reported uncertainties in the last significant digit of fitted parameters are shown in parentheses.

Key: Number of TOAs (N_{toa}), Root mean squared (RMS), Reduced chi-squared (χ^2_{red})

a three month gap in the CHIME data. NG15 observations across the time period of this analysis are also relatively higher cadence than the usual monthly cadence (Figure 3). The gap in CHIME data combined with the higher cadence NG15 data makes it appear that there are comparable numbers of CHIME vs NG15 TOAs, but when this analysis is extended beyond the overlap period of this analysis, we predict that the ratio of CHIME to NG15 TOAs will be comparable to what we see for PSR J0613-0200 and PSR J2145-0750. The weighted TOA RMS is approximately 0.016% of the pulsar spin period and the weighted DM RMS is 0.0016% of the fiducial DM. The timing ephemeris had 529 degrees of freedom with a χ^2_{red} of 1.040.

PSR J2145–0750 is a 16.05-ms MSP in a 6.84-day circular orbit about a $0.86 \pm 0.0015 M_{\odot}$ white dwarf companion initially discovered using the Parkes Telescope (Bailes et al., 1994; Deller et al., 2016). CHIME TOAs for this source show more scattering and, on average, much higher uncertainties than NG15 TOAs. We also see more scattering in the NG15 DM residuals vs CHIME (Figure 4). The timing ephemeris had 275 degrees of freedom with a χ^2_{red} of 1.752, suggesting our timing model may be somewhat underfitted. The weighted TOA RMS is approximately 0.0058% of the measured spin period and the weighted DM RMS is 0.0024% of the fiducial DM.

4. Conclusions and Future Work

For all four sources our timing RMS values were a very small fraction of the respective pulsar spin periods, which is important for doing high precision pulsar timing (Table 1). We also saw that our DM RMS's were very low percentages of the fiducial DM's which tells us that our models of time-varying DM are accurate. Three of our sources had a χ^2_{red} close to 1 or nearly 1. PSR J2145–0750 had a slightly higher χ^2_{red} of 1.752 which is still close to 1, suggesting the timing model is still describing the data fairly well. The higher χ^2_{red} could be due to unmodeled timing noise or underestimating uncertainties.

Measurements of spin and binary parameters, where applicable, are broadly consistent with values published in NG15 albeit with larger uncertainties (Agazie, Alam, et al., 2023). This is once again likely a limitation induced by the relatively short timing baseline use in this analysis. We predict that a full-scale analysis on the entire NG15 and CHIME timing baselines will produce more precise measurements of spin and binary parameters than published in NG15.

In nearly all of the timing residual plots it is clear that the CHIME TOAs, on average, have increased uncertainties compared to many of the NG15 TOAs. Some of this can be attributed to CHIME operating at lower frequencies than

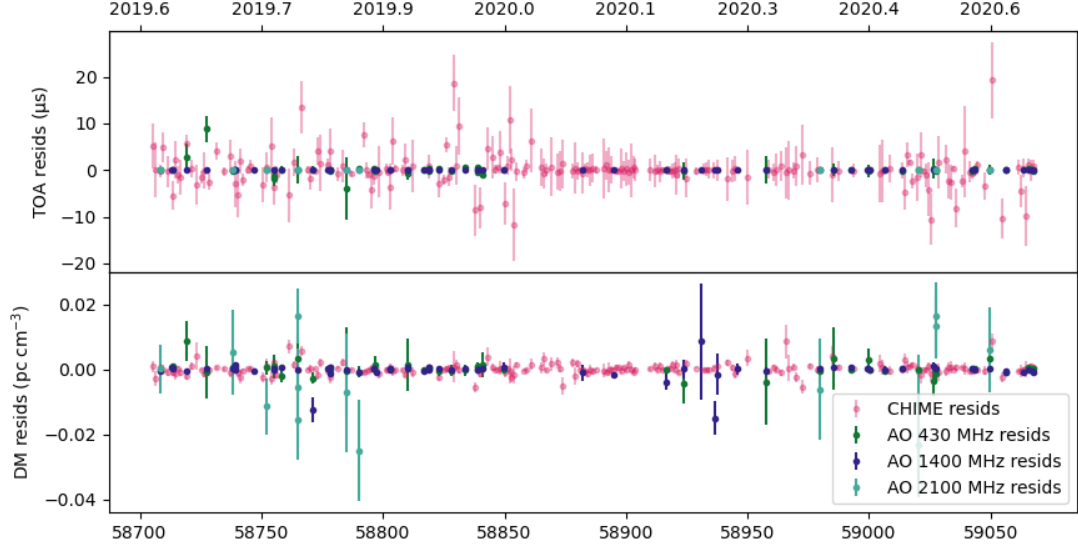


Figure 1: Top panel: TOA vs timing residuals with error bars for PSR J0030+0451. Bottom panel: Corresponding DM measurements vs DM residuals with error bars. The bottom axis represents measurements in both panels in MJD and the top in units of years. Green, navy, and turquoise points represent AO data taken at 430 MHz, 1400 MHz, and 2100 MHz respectively. CHIME data is in pink.

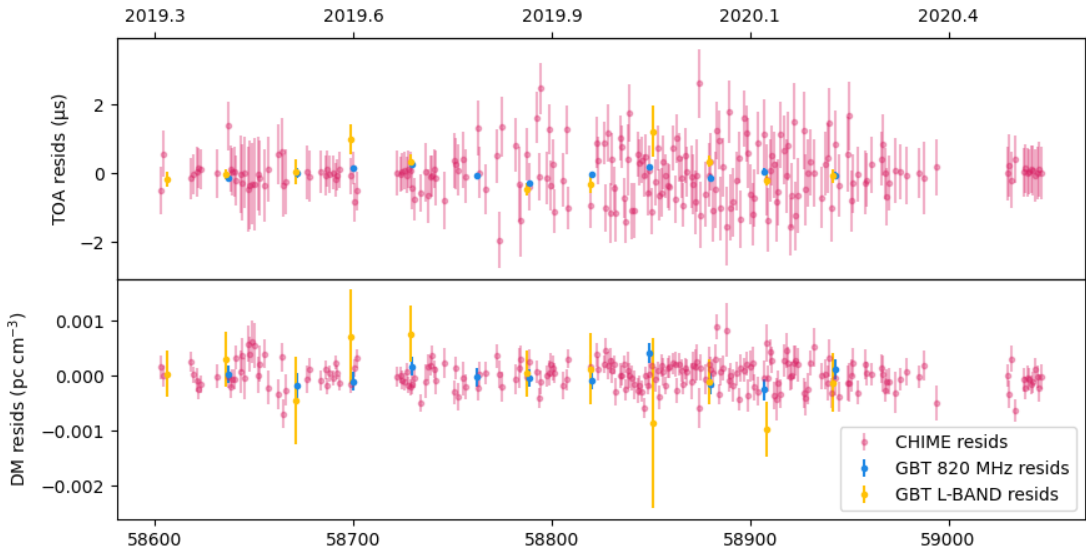


Figure 2: Top panel: TOA vs timing residuals with error bars for PSR J0613-0200. Bottom panel: Corresponding DM measurements vs DM residuals with error bars. The bottom axis represents measurements in both panels in MJD and the top in units of years. Blue and yellow points represent GBT data taken at 820 MHz and 1400 MHz respectively. CHIME data is in pink.

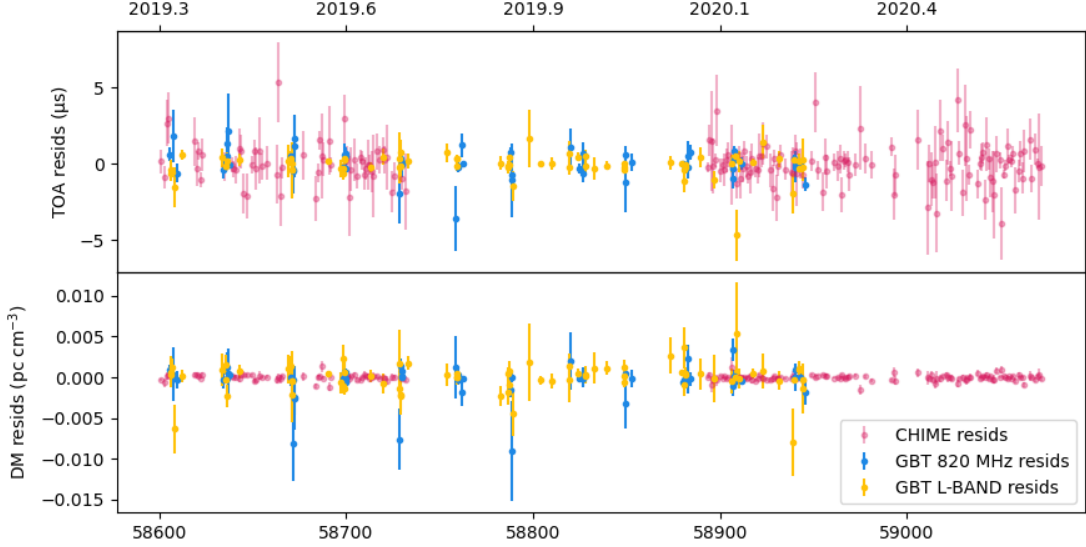


Figure 3: Top panel: TOA vs timing residuals with error bars for PSR J0740+6620. Bottom panel: Corresponding DM measurements vs DM residuals with error bars. The bottom axis represents measurements in both panels in MJD and the top in units of years. Blue and yellow points represent GBT data taken at 820 MHz and 1400 MHz respectively. CHIME data is in pink.

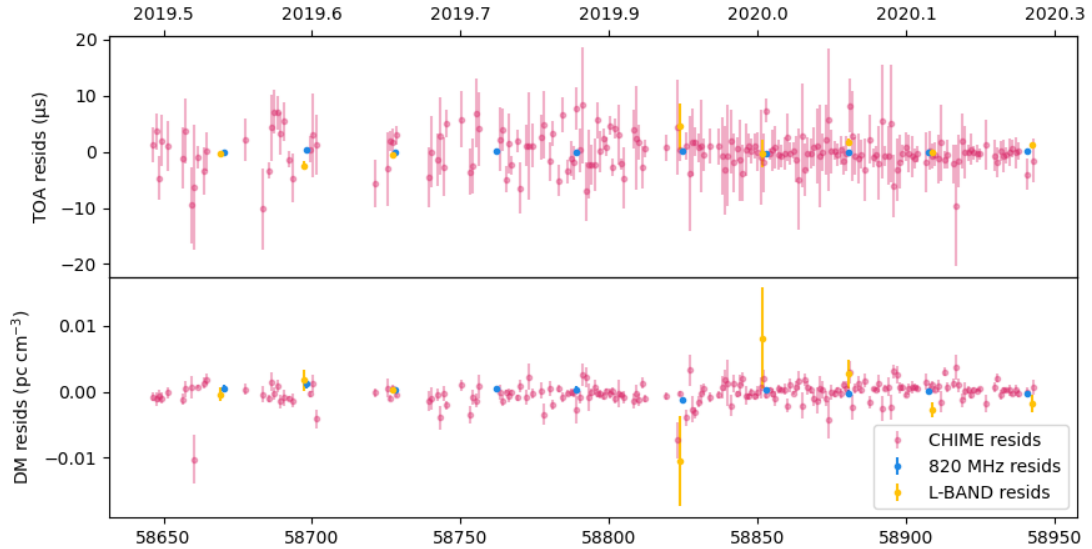


Figure 4: Top panel: TOA vs timing residuals with error bars for PSR J2145–0750. Bottom panel: Corresponding DM measurements vs DM residuals with error bars. The bottom axis represents measurements in both panels in MJD and the top in units of years. Blue and yellow points represent GBT data taken at 820 MHz and 1400 MHz respectively. CHIME data is in pink.

nearly all the receivers used for NG15, except for the AO 430 MHz receiver. TOA uncertainty scales as $\nu^{-1/2}$, so we would generally expect high-frequency TOAs to have smaller error bars. The CHIME telescope also has a lower gain than the GBT, and gain is inversely proportional to TOA uncertainty (Lorimer, 2008; Lorimer & Kramer, 2012).

Our RFI excision approach to remove bad channels after frequency and time averaging has the potential to cause us to lose a significant percentage of frequency information. For PSR J0030+0451 and PSR J0613-0200 more than 50% of the total frequency coverage was unusable due to RFI. Another compounding factor is that parts of the CHIME observing band are unprotected for radio astronomy as they overlap with frequencies used for cell phones. Thus, CHIME has an extremely variable RFI environment and continuing work must be done to make an automated RFI excision algorithm.

The next steps of this analysis will be to extend it to the entire NG15 and CHIME timing baseline, and to look at measurements of astrometric and PK parameters. For the three binary pulsars in our analysis, we will examine how our constraints of companion and pulsar masses compare to those in published literature. The timing baseline of CHIME is roughly four years and thus will be long enough to make independent measurements of some astrometric and PK parameters.

Acknowledgments

The National Radio Astronomy Observatory and Green Bank Observatory are facilities of the National Science Foundation operated under cooperative agreement by Associated Universities, Inc.

We acknowledge that CHIME is located on the traditional, ancestral, and unceded territory of the Syilx/Okanagan people. We are grateful to the staff of the Dominion Radio Astrophysical Observatory, which is operated by the National Research Council of Canada. CHIME is funded by a grant from the Canada Foundation for Innovation (CFI) 2012 Leading Edge Fund (Project 31170) and by contributions from the provinces of British Columbia, Québec and Ontario. The CHIME/FRB Project, which enabled development in common with the CHIME/Pulsar instrument, is funded by a grant from the CFI 2015 Innovation Fund (Project 33213) and by contributions from the provinces of British Columbia and Québec, and by the Dunlap Institute for Astronomy and Astrophysics at the University of Toronto. Additional support was provided by the Canadian Institute for Advanced Research (CIFAR), McGill University and the McGill Space Institute thanks to the Trottier Family Foundation, and the University of British Columbia. The CHIME/Pulsar instrument hardware was funded by NSERC RTI-1 grant EQPEQ 458893-2014.

This research was enabled in part by support provided by the BC Digital Research Infrastructure Group and the Digital Research Alliance of Canada (alliancecan.ca).

This work was supported by NASA under Award No. RFP23_1-0 through the Wisconsin Space Grant Consortium Graduate and Professional Research Fellowship.

References

Agazie, G., Alam, M. F., Anumarpudi, A., Archibald, A. M., Arzoumanian, Z., Baker, P. T., ... Nanograv Collaboration (2023, July). The NANOGrav 15 yr Data Set: Observations and Timing of 68 Millisecond Pulsars. , 951(1), L9. doi: 10.3847/2041-8213/acda9a

Agazie, G., Anumarpudi, A., Archibald, A. M., Arzoumanian, Z., Baker, P. T., Bécsy, B., ... Nanograv Collaboration (2023, July). The NANOGrav 15 yr Data Set: Evidence for a Gravitational-wave Background. , 951(1), L8. doi: 10.3847/2041-8213/acdac6

Alam, M. F., Arzoumanian, Z., Baker, P. T., Blumer, H., Bohler, K. E., Brazier, A., ... Nanograv Collaboration (2021a, January). The NANOGrav 12.5 yr Data Set: Observations and Narrowband Timing of 47 Millisecond Pulsars. *The Astrophysical Journal Supplement*, 252(1), 4. doi: 10.3847/1538-4365/abc6a0

Alam, M. F., Arzoumanian, Z., Baker, P. T., Blumer, H., Bohler, K. E., Brazier, A., ... Nanograv Collaboration (2021b, January). The NANOGrav 12.5 yr Data Set: Wideband Timing of 47 Millisecond Pulsars. *The Astrophysical Journal Supplement*, 252(1), 5. doi: 10.3847/1538-4365/abc6a1

Arzoumanian, Z., Baker, P. T., Blumer, H., Bécsy, B., Brazier, A., Brook, P. R., ... Nanograv Collaboration (2020, December). The NANOGrav 12.5 yr Data Set: Search for an Isotropic Stochastic Gravitational-wave Background. *The Astrophysical Journal Letters*, 905(2), L34. doi: 10.3847/2041-8213/abd401

Bailes, M., Harrison, P. A., Lorimer, D. R., Johnston, S., Lyne, A. G., Manchester, R. N., ... Robinson, C. (1994, April). Discovery of Three Binary Millisecond Pulsars. , 425, L41. doi: 10.1086/187306

Burgio, G. F., Schulze, H. J., Vidaña, I., & Wei, J. B. (2021, September). Neutron stars and the nuclear equation of state. *Progress in Particle and Nuclear Physics*, 120, 103879. doi: 10.1016/j.ppnp.2021.103879

CHIME/Pulsar Collaboration, Amiri, M., Bandura, K. M., Boyle, P. J., Brar, C., Cliche, J. F., ... Wang, X. (2021, July). The CHIME Pulsar Project: System Overview. , 255(1), 5. doi: 10.3847/1538-4365/abfdcb

Deller, A. T., Vigeland, S. J., Kaplan, D. L., Goss, W. M., Brisken, W. F., Chatterjee, S., ... Lyne, A. (2016, September). Microarcsecond VLBI Pulsar Astrometry with PSR π . I. Two Binary Millisecond Pulsars with White Dwarf Companions. , 828(1), 8. doi: 10.3847/0004-637X/828/1/8

Fonseca, E., Cromartie, H. T., Pennucci, T. T., Ray, P. S., Kirichenko, A. Y., Ransom, S. M., ... Zhu, W. W. (2021, July). Refined Mass and Geometric Measurements of the High-mass PSR J0740+6620. *The Astrophysical Journal Letters*, 915(1), L12. doi: 10.3847/2041-8213/ac03b8

Freire, P. C. C., & Wex, N. (2010, November). The orthometric parametrization of the Shapiro delay and an improved test of general relativity with binary pulsars. , 409(1), 199-212. doi: 10.1111/j.1365-2966.2010.17319.x

Good, D. C. (2021). *Timing pulsars and detecting radio transients with chime* (Doctoral dissertation, University of British Columbia). doi: <http://dx.doi.org/10.14288/1.0401783>

Lange, C., Camilo, F., Wex, N., Kramer, M., Backer, D. C., Lyne, A. G., & Doroshenko, O. (2001, September). Precision timing measurements of PSR J1012+5307. , 326(1), 274-282. doi: 10.1046/j.1365-8711.2001.04606.x

Lommen, A. N., Zepka, A., Backer, D. C., McLaughlin, M., Cordes, J. M., Arzoumanian, Z., & Xilouris, K. (2000, December). New Pulsars from an Arecibo Drift Scan Search. , 545(2), 1007-1014. doi: 10.1086/317841

Lorimer, D. R. (2008, November). Binary and Millisecond Pulsars. *Living Reviews in Relativity*, 11(1), 8. doi: 10.12942/lrr-2008-8

Lorimer, D. R., & Kramer, M. (2012). *Handbook of Pulsar Astronomy*. Cambridge University Press.

Lorimer, D. R., Nicastro, L., Lyne, A. G., Bailes, M., Manchester, R. N., Johnston, S., ... Harrison, P. A. (1995, February). Four New Millisecond Pulsars in the Galactic Disk. , 439, 933. doi: 10.1086/175230

Luo, J., Ransom, S., Demorest, P., Ray, P. S., Archibald, A., Kerr, M., ... Jenet, F. A. (2021, April). PINT: A Modern Software Package for Pulsar Timing. , 911(1), 45. doi: 10.3847/1538-4357/abe62f

NANOGrav Collaboration, Arzoumanian, Z., Brazier, A., Burke-Spolaor, S., Chamberlin, S., Chatterjee, S., ... Zhu, W. (2015, November). The NANOGrav Nine-year Data Set: Observations, Arrival Time Measurements, and Analysis of 37 Millisecond Pulsars. *The Astrophysical Journal*, 813(1), 65. doi: 10.1088/0004-637X/813/1/65

Pennucci, T. T. (2019, January). Frequency-dependent Template Profiles for High-precision Pulsar Timing. *The Astrophysical Journal Supplement*, 871(1), 34. doi: 10.3847/1538-4357/aaef

Stovall, K., Lynch, R. S., Ransom, S. M., Archibald, A. M., Banaszak, S., Biwer, C. M., ... Wells, B. L. (2014, August). The Green Bank Northern Celestial Cap Pulsar Survey. I. Survey Description, Data Analysis, and Initial Results. , 791(1), 67. doi: 10.1088/0004-637X/791/1/67

The CHIME Collaboration, Amiri, M., Bandura, K., Boskovic, A., Chen, T., Cliche, J.-F., ... Wulf, D. (2022, January). An Overview of CHIME, the Canadian Hydrogen Intensity Mapping Experiment. *arXiv e-prints*, arXiv:2201.07869.

van Straten, W., Demorest, P., & Ostrowski, S. (2012). *Pulsar data analysis with psrchive*.